



ELSEVIER

Available online at www.sciencedirect.com

Journal of Pharmaceutical and Biomedical Analysis

xxx (2003) xxx–xxx

JOURNAL OF
PHARMACEUTICAL
AND BIOMEDICAL
ANALYSISwww.elsevier.com/locate/jpba

Near-infrared spectroscopy for the determination of testosterone in thin-film composites

William Fountain^a, Karen Dumstorf^b, Amanda E. Lowell^{a,b},
Robert A. Lodder^{a,b}, Russell J. Mumper^{a,*}

^a Division of Pharmaceutical Sciences, Center for Pharmaceutical Science and Technology, College of Pharmacy, University of Kentucky, Lexington, KY 40536-0082, USA

^b Department of Chemistry, University of Kentucky, Lexington, KY 40536-0082, USA

Received 12 July 2002; accepted 19 March 2003

Abstract

More rapid, reproducible, and cost-effective methods to control product quality in the pharmaceutical industry continue to be a major emphasis, particularly with the FDA through its recent process analytical technologies (PAT) initiative. Many different methods have been used to determine the stability and content uniformity of a drug in various dosage forms; however, most of these methods include the destruction of the sample. Therefore, the development of nondestructive methods that allow the analysis of each individual dosage form has become the basis of much research. A new assay for the nondestructive determination of testosterone content in mucoadhesive bi-layer thin-film composites (TFCs) using near-infrared spectroscopy (NIR) was developed. Five sets of the circular films ($n = 5$) with theoretical testosterone content of 0, 1, 2, 3, and 4 mg per 3/8th in. diameter disks were scanned in the near-infrared region of 1100–2500 nm to determine testosterone content. The NIR results were directly compared with those obtained using a previously developed ultraviolet assay for testosterone at 240 nm. Principal component regression (PCR) was performed to calibrate the NIR assay. This correlation produced $r^2 = 0.99$ with a standard error of estimate (SEE) = 0.18 mg, and a standard error of performance (SEP) = 0.18 on cross validation with an equal number of samples (F test passed at $P = 0.05$). Though the UV assay showed a slightly better r^2 value, the NIR assay was much quicker, easier, and nondestructive. Therefore, the NIR assay may have significant potential for use in the quality control of pharmaceutical films containing drugs.

© 2003 Published by Elsevier B.V.

Keywords: Principal component regression; Buccal; Mucoadhesive; Analytical method; Nondestructive

* Corresponding author. Tel.: +1-859-257-2300x258; fax: +1-859-323-5985.

E-mail address: rjmump2@uky.edu (R.J. Mumper).

1. Introduction

The pharmaceutical industry has been rapidly expanding into new and different types of delivery vehicles in the past decade. Many of these new delivery methods are presenting unique problems concerning the quality control of these products. Two of the most important parameters in the quality control of dosage forms are drug stability and content uniformity. The most common methods for determining stability and content uniformity involve the first step of dissolving the sample in a suitable medium. A multitude of analytical techniques can then be used to determine the drug concentration and/or stability. Some commonly used techniques are HPLC, gas chromatography (GC), capillary electrophoresis (CE), and ultraviolet (UV) analysis. All of these analytical methods require destruction of the sample in combination with a series of physical and/or chemical manipulations. For example, sample preparations can be very difficult and tedious due to multiple dilutions, filtrations and extractions. Moreover, depending on the analytical method employed, such techniques often require lengthy analysis times for each sample.

The development of more rapid, reproducible, cost-effective, and perhaps non-destructive methods to quality control products in the pharmaceutical industry continues to be a major emphasis. A potential method that may meet this criteria is near infrared spectroscopy (NIR) [1–5]. NIR is performed over a range of wavelengths that is capable of both quantitative and qualitative analysis. One important feature of NIR is that it can be performed on the raw product without destroying the sample. Secondly, the sample time can be reduced to only a few minutes per sample. Many companies that make solid dosage forms are turning to NIR analysis for quality control of their products. For example, utilizing NIR, a manufacturer of solid tablets may randomly sample from a population of tablets during a production run and quickly determine, in real time, whether the batch falls within acceptable limits for drug content and/or content uniformity. In fact, the Food and Drug Administration has strongly encouraged the use of NIR as on-line,

in-line, or at-line measurement tool for unit operations and/or as an alternative test [6].

NIR spectrometry and nonparametric multivariate analysis are a strong combination in solid dosage-form analysis, as demonstrated by analysis of intact tablets [7], detection of tampering in gelatin capsules [8], and detection of contamination in drug capsules [9]. NIR spectrometry and multivariate analysis has been further employed to discriminate between different tablet formulations inside blister packages [10]. NIR spectrometry and multivariate analysis have even been used to determine the moisture and salicylic acid content of degraded aspirin tablets [11].

Raman spectrometry with a NIR light source has also been used on drug formulations in gel capsules and on gel capsules inside blister packs [12]. Analysis of the Raman spectra collected from bucindolol capsules in the interior of the blister packs with multivariate calibration yielded a standard error of performance (SEP) of only 3.36% of the range of active ingredient. As is frequently the case in NIR reflectance spectrometry, the largest source of prediction error was sample inhomogeneity.

NIR cameras are being increasingly employed in hyperspectral imaging experiments. Imaging spectrometers based on framing array cameras have rapid scanning ability and high sensitivity. NIR imaging has been used in human stroke patients to discover atherosclerotic plaque by identifying the location of oxidized lipoprotein spectral signatures [13]. The InSb camera employed in these studies had a custom cold (77 K) bandpass filter for NIR use and could be fitted with a warm (298 K) tunable interference filter system or a warm filter disk. Probability density contours drawn in multi-dimensional standard deviations (S.D.s) were put to use to form pictures that exposed the locations of atherosclerotic plaque inside blood vessels. NIR multispectral imaging has been used to monitor solid-phase peptide synthesis [14]. An acousto-optic tunable filter and a NIR indium gallium arsenide (InGaAs) focal plane array camera maintained all the advantages of a traditional NIR spectrometer in noninvasive observation of reactions and identification of the products during the solid-phase peptide synthesis. The NIR hyperspec-

80
81
82
83
84
85
86
87
88
89
90
91
92
93
94
95
96
97
98
99
100
101
102
103
104
105
106
107
108
109
110
111
112
113
114
115
116
117
118
119
120
121
122
123
124
125
126
127

128 tral imaging system added an important character-
129 istic to the monitoring that traditional NIR
130 spectrometers could not offer the ability to mea-
131 sure spectra at different sites within a sample. In
132 the peptide synthesis study, spectra recorded by
133 16×16 pixels were pooled to calculate an average
134 spectrum for each sample. However, a qualitative
135 spectrum could be gathered from a single pixel.

136 The kinetics of curing of an epoxy resin by
137 amine was also studied using a NIR hyperspectral
138 imaging spectrometer [15]. The kinetics of curing
139 was calculated from data collected by a single pixel
140 in the camera. The reaction rates inside the sample
141 were not uniform. Because of this kinetic inhomog-
142 eneity, differences in the degree of cure at
143 different positions within the sample were as high
144 as 37% when data from just a single pixel were
145 employed for calculation. The inhomogeneity was
146 not observed if the average of a large number of
147 pixels were used. In a similar manner, ethylene/
148 vinyl acetate copolymers were shown to display a
149 high degree of chemical inhomogeneity [16].

150 Our laboratories have studied the potential of
151 NIR to detect and quantify drug content and
152 content uniformity of drugs in novel mucoadhesive
153 bi-layer thin-film composites (TFCs) [17–19].
154 These bioerodable TFCs (~ 100 – $200 \mu\text{m}$ in total
155 thickness) are comprised of two layers, a drug
156 containing mucoadhesive polymer layer, and an
157 impermeable layer consisting of a pharmaceutical
158 wax. The TFCs strongly adhere to a wet mucosal
159 surface (i.e. buccal tissue) for up to 4 h and allow
160 for uni-directional drug delivery through the tissue
161 into the systemic circulation, or local delivery of
162 mucosal vaccines. Recently, these TFCs have been
163 used to deliver testosterone, salmon calcitonin,
164 and (genetic) vaccines by the buccal routes in
165 rabbits [17–19]. The current method to quantify
166 testosterone content in the TFCs is destructive and
167 time consuming involving the dissolution of the
168 films containing testosterone in ethanol overnight
169 followed by subsequent dilution with additional
170 ethanol, filtration, and assay by UV.

171 The overall goal of this work was to develop a
172 rapid, reproducible, and cost-effective quality
173 control method for testosterone in the TFCs by
174 employing NIR analysis.

2. Experimental 175

2.1. Materials 176

Polycarbophil (Noveon[®] AA-1, USP) was a 177
generous gift from BF Goodrich (Cleveland, 178
OH). Polymethacrylic acid-co-methyl methacry- 179
late (Eudragit S-100) was obtained from Röhm 180
America Inc. (Piscataway, NJ). Testosterone (4- 181
androsten-17 β -ol-3-one) was purchased from Al- 182
drich Chemicals (Milwaukee, WI). DENTSPLY[®] 183
Utility Wax was obtained from DENTSPLY 184
International (York, PA). Ethanol (95%) USP, 185
was purchased from Spectrum Laboratory Pro- 186
ducts (Gardena, CA). 187

2.2. Preparation of thin-film composites [17–19] 188

The mucoadhesive TFCs were first produced as 189
a semi-viscous gel and poured into molds and 190
dried. Briefly, 95% ethanol USP (90.0 g), was 191
added to a 300 ml stainless steel beaker. A 192
Caframo Mixer (Model BDC 1850; Warton, 193
Ontario) equipped with a 3 cm diameter dispersion 194
blade was lowered into the solution and stirring 195
was set at 250 rpm. Eudragit S-100 (1.333 g) was 196
added to the solution over a period of 5 min and 197
the solution turned an opaque bluish color. The 198
solution was allowed to stir until the solution 199
became clear. Next, Noveon[®] AA1 (4.0 g) was 200
slowly added in small portions over 30 min. The 201
gel was then stirred at 1000 rpm for 6 h and then 202
q.s. to 100 g with 95% ethanol. The finished 203
placebo gel was considered to be a stock placebo 204
gel ($1.333 \times$). 205

Gels containing testosterone were then prepared 206
by aliquoting five separate stock placebo gels (15 g 207
each) into separate 40 ml wide mouth I-Chem glass 208
jars. The following accurately weighed testostero- 209
ne powder was then added to each respective 210
stock placebo gels stirring at 600 rpm; 0.0, 0.1803, 211
0.3606, 0.5409 and 0.7212 g. The gels containing 212
testosterone were mixed until all of the testostero- 213
ne was dissolved in the gel at which point the gels 214
were made to 20 g with 95% ethanol. The gels 215
containing testosterone were cast into films by first 216
fixing a plastic circular hollow ring (diameter = 6.2 217
cm; total area = 30.175 cm^2) onto a 4 in. \times 4 in. 218

219 Mylar film. A volume of 7 ml of each gel was
 220 dispensed from a 10 ml glass serological pipette
 221 into the middle of the circular ring. The gels were
 222 then dried overnight in an oven at a temperature
 223 of 55 °C. Once dry, the plastic ring was removed
 224 and the side of the film containing the muco-
 225 adhesive film was rapidly dipped into melted
 226 Dentsply wax and removed. The TFCs were
 227 allowed to cool and then detached from the Mylar
 228 film. A 3/8 in. Arch Punch (C.S. Osborne;
 229 Harrison, NJ) was used to cut out circular disks
 230 containing a theoretical testosterone dose of 0, 1,
 231 2, 3, or 4 mg. The thickness and weight of placebo
 232 TFCs and TFCs containing testosterone (n = 10)
 233 were determined. A Marathon Electronic Digital
 234 Micrometer Model 030025 EMD (0–25 mm,
 235 resolution of 0.001 mm) was used to determine
 236 the thickness of films.

237 2.3. Near infrared analysis of films

238 A Technicon InfraAlyzer 500 (Tarrytown, NY)
 239 was used to obtain NIR spectra of all film samples.
 240 Each concentration of testosterone stated above
 241 was formed into 3/8 in. disks (n = 5) and assayed
 242 by NIR separately. The scan was performed in the
 243 range of 1100–2500 nm. The samples were
 244 scanned using an aluminum sample focusing-cup
 245 with a 135° liquid insert [20]. The entire sample
 246 area was illuminated. A glass cover slip was placed
 247 over the liquid insert and secured in place by black
 248 electrical tape. Each disk was placed on top of the
 249 glass cover slip and placed inside the spectro-
 250 photometer. Each sample required a minute for
 251 the sample placement and approximately 2 min for
 252 the scan. One complete scan was obtained in 2 min
 253 with 170-ms total signal integration at each
 254 wavelength. Multiplicative scatter correction was
 255 applied to the collected spectra of the films to
 256 reduce the effect of any variations in film thickness
 257 on the results. After each disk was scanned, it was
 258 placed in a clean 7-ml scintillation vial and clearly
 259 labeled.

260 2.4. Ultraviolet (UV) assay of the TFCs

261 A Beckman Instruments Model DU-7500i Spec-
 262 trophotometer (Fullerton, CA) was used for UV

analysis of samples. After the NIR spectrum was 263
 obtained for each disk, 1 ml of 95% ethanol was 264
 added to each capped vial. The vials were then 265
 vigorously shaken over night to ensure complete 266
 dissolution of the films in the ethanol. The 267
 solutions were diluted to a theoretical concentra- 268
 tion of 20 mg/ml with ethanol and filtered using a 269
 0.22 mm PTFE syringe filter to remove polymers 270
 and wax. The UV absorbance was determined at 271
 240 nm using the diode-array spectrophotometer. 272
 The absorbance values were compared with a 273
 standard curve of testosterone in ethanol ranging 274
 from 1.5625 to 25 mg/ml. The results of the UV 275
 assay were used to calculate the concentration of 276
 testosterone in the film according to the dilution 277
 factor. 278

279 2.5. Data correlation and analysis

In NIR spectrometry, the absorbance at any 280
 single wavelength contains contributions from 281
 many different sources (different analytes, physical 282
 configurations of the sample, etc.). For this reason 283
 any single wavelength in the spectrum may not 284
 present a reliable linear correlation between the 285
 absorbance and testosterone content. Therefore, 286
 the statistical method of principal component 287
 regression (PCR) was performed in order to 288
 extract the testosterone concentration data from 289
 the spectra. 290

The actual sample testosterone concentrations 291
 according to the UV assay were paired with their 292
 corresponding NIR spectra. PCR was employed to 293
 analyze the spectra of intact films [11]. PCR uses 294
 transformation of the spectra to principal axes to 295
 convert the spectral absorbance values into princi- 296
 pal component “scores” (coordinates in the new 297
 PC coordinate system). Multiple linear regression 298
 of the PC scores and testosterone concentrations is 299
 used to create a calibration function for determin- 300
 ing testosterone concentrations from spectra of 301
 new unknown films. Principal-axis transformation 302
 (PAT) of the spectra in **T** begins with standardiz- 303
 ing the spectral data by subtracting the mean 304
 absorbance of each column $\mu(t_j)$ from the absor- 305
 bances in each column t_{ij} , and dividing the 306
 difference by the corresponding standard deviation 307
 $\sigma_{S.D.}(t_j)$: 308

$$309 \quad \mathbf{Z}_{ij} = [t_{ij} - \mu(t_j)] / \sigma_{S.D.}(t_j) \quad (1)$$

310 The normalized spectral matrix \mathbf{Z} is then trans-
 311 posed and retained until the transformation matrix
 312 is formed. Normalization gives information at
 313 each wavelength equal weight in the post-trans-
 314 formation spectral hyperspace. The transforma-
 315 tion matrix \mathbf{L}^{-1} is formed from the eigenvalues λ
 and eigenvalues \mathbf{X}_λ of a correlation matrix \mathbf{R} :

$$316 \quad r_{jk} = \sum_{i=1}^n [t_{ij} - \mu(t_j)] \\ \times [t_{ik} - \mu(t_k)] / (n-1) \sigma_{S.D.}(t_j) \sigma_{S.D.}(t_k) \quad (2)$$

317 where n is the number of sample spectra and \mathbf{R} is
 318 defined from $k = 1$ to the number of columns in \mathbf{T} .
 319 The square roots of the eigenvalues λ of \mathbf{R} are used
 320 to diagonalize a square matrix. The matrix pro-
 321 duct of the square root of these eigenvalues and \mathbf{X}_λ
 322 gives \mathbf{L} , which turns into the transformation
 323 matrix upon inversion. The transformation matrix
 324 effectively serves as a map joining the primary
 325 spectral hyperspace to the new hyperspace, which
 326 is ordinarily of smaller dimension. New spectral
 327 coordinates, supplied in principal-axis space for
 the sample spectra in \mathbf{T} , are given by:

$$328 \quad \mathbf{T}_p = \mathbf{L}^{-1} \mathbf{Z} \quad (3)$$

329 The new spectra are employed to good effect in
 330 both qualitative and quantitative analysis of a
 331 sample through application of least-squares re-
 332 gression and discriminant analysis techniques. The
 333 PAT process eliminates the collinearity problem in
 334 the NIR spectra of samples, and reduces (often to
 335 less than one-half dozen) the effective number of
 336 wavelengths (dimensions in hyperspace) that need
 337 to be taken into account in qualitative and
 qualitative analysis of samples.

338 3. Results and discussion

339 Testosterone is most commonly used to treat
 340 male hypogonadism, which is characterized by
 341 delayed puberty, aplastic anemia, or protein wast-
 342 ing diseases as well as diminished libido, depressed
 343 mood, low energy, and depleted muscle mass [21–
 344 23]. There are currently several marketed products

345 of testosterone indicated for androgen replacement
 346 therapy including intramuscular oil-based depot
 347 injections, transdermal systems, oral tablets, and
 348 sublingual tablets [24–30]. The oral bioavailability
 349 of testosterone has been reported to be from 1 to
 350 6% due to extensive first pass metabolism and low
 351 aqueous solubility [24,29]. The solubility of testos-
 352 terone in water at 37 °C is only 46.3 µg/ml [24].
 353 There are currently three marketed transdermal
 354 products for delivering from 2.5 to 6 mg testoster-
 355 one. However, these patches are as large as 44 cm²
 356 and have been reported to cause skin irritation in
 357 as high as 60% of patients due to the inclusion of
 358 penetration enhancers [30–32]. Due to these limit-
 359 ing factors, buccal delivery of testosterone may be
 360 a plausible approach.

361 In previous studies in rabbits using TFCs
 362 containing testosterone, Jay et al. reported that
 363 the relative bioavailability for rabbits treated with
 364 the testosterone (4 mg) TFCs was 50.2 ± 3.2% with
 365 a CV of 6.4% [17]. It was concluded that these bi-
 366 layer mucoadhesive TFCs disks could deliver
 367 physiologically relevant amounts of insoluble
 368 drugs such as testosterone across the buccal
 369 mucosa.

370 In these current studies, the results from the
 371 mass and thickness measurements showed that the
 372 placebo TFCs had an average weight of 9.96 ± 1
 373 mg and a thickness of 109 ± 6 µm. TFCs contain-
 374 ing 4 mg testosterone had an average weight of
 375 14 ± 2.6 mg and a thickness of 186 ± 34 µm. These
 376 results confirmed that the manufacturing process
 377 for the TFCs produced films having suitable
 378 weight and thickness uniformity for these studies.

379 The UV assay was developed by first scanning a
 380 solution of 12.5 mg of testosterone per ml of
 381 ethanol over a range of 190–300 nm. The resulting
 382 spectrum is shown in Fig. 1. The peak absorbance
 383 was found at 240 nm and this value was used in the
 384 formation of a standard curve. The standards were
 385 in the range of 1.563–25 mg/ml resulting in $r^2 =$
 386 0.999 by least squares regression as shown in Fig.
 387 2. In order for the amount of testosterone on the
 388 disks to be quantified, they were dissolved in
 389 ethanol and diluted to a theoretical concentration
 390 of 20 mg/ml in ethanol. The absorbance of these
 391 samples were determined at 240 nm and compared
 392 with the standard curve. The actual quantity of

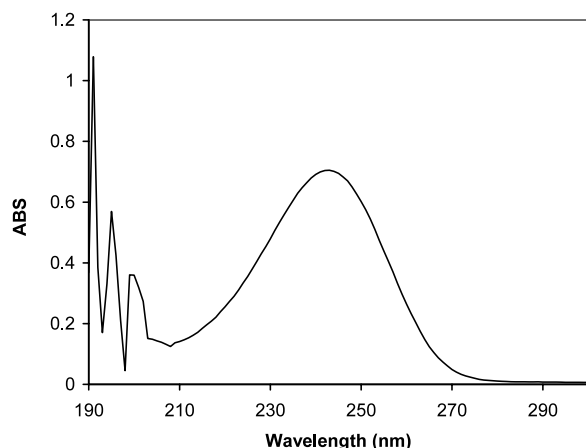


Fig. 1. UV spectrum of extracted testosterone from 3/8 in. TFCs.

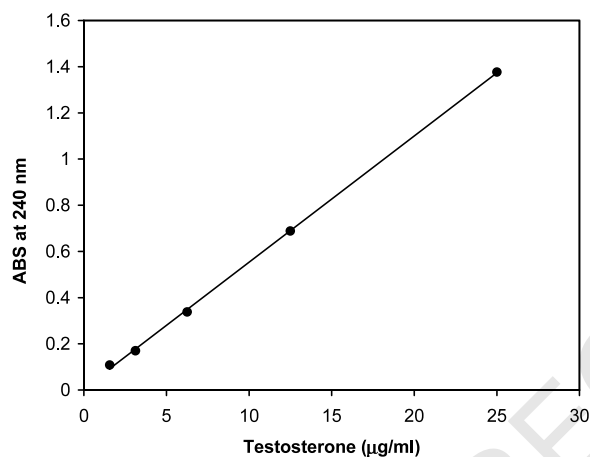


Fig. 2. UV standard curve of testosterone (1.5625–25 mg/ml) in ethanol.

393 testosterone in each disk was determined according to the standard curve and the dilution factor.
394 The resulting testosterone weights for each of the
395 corresponding TFCs are listed in Table 1. The
396 results for the UV analysis for testosterone content
397 uniformity demonstrate that the UV assay was
398 suitable for meeting content uniformity require-
399 ments, with R.S.D. values between 3 and 9% for
400 TFCs containing 1, 2, or 3 mg of testosterone per
401

3/8 in. disk. Further, the corresponding label 402
strengths for testosterone in the TFCs were in 403
the usually accepted limits of 90–110% except for 404
the TFCs containing 3 mg testosterone. For 405
reasons not known, TFCs containing 3 mg testos- 406
terone had average label strengths of 3.7 mg, 407
which could not be explained by improper testos- 408
terone concentrations in the initial gels used to 409
manufacture the TFCs. In general, these present 410
results for testosterone content uniformity in 411
TFCs containing testosterone agreed well with 412
previous results [17]. 413

The NIR of the disks containing testosterone 414
were analyzed by first subtracting the spectrum of 415
a background scan from each measurement. The 416
resulting corrected NIR spectra are shown in Fig. 417
3. The univariate correlations by wavelength to 418
testosterone concentration ranged from -0.96 to 419
 $+0.98$. It is well known that calibrations created 420
using a single wavelength are often not useful in 421
mixtures of many constituents, however, and for 422
that reason NIR spectrometry employs multivariate 423
calibration techniques. PCR was performed on 424
the NIR spectra and testosterone concentrations 425
as determined by the UV assay. Four PCs were 426
used in the calibration. The resulting concentra- 427
tions of testosterone in each disk that were 428
determined by the PCR were correlated with the 429
concentrations found in the UV assay. The correla- 430
tion ($r^2 = 0.99$) is shown in Fig. 4. Cross valida- 431
tion was performed by applying the calibration 432
developed on the training samples to the same 433
number of additional samples that were not used 434
to develop the calibration. The validation samples 435
also covered the concentration range from 0 to 4 436
mg. The standard error of estimate (SEE) = 0.18 437
mg on the calibration samples, and the SEP = 0.18 438
mg on the validation samples, verifying cross 439
validation by the F test at $P = 0.05$. The 440
R.S.D. = 5% and the detection limit (three times 441
the S.D. of the blank) = 0.50 mg. The R.S.D. of 442
the NIR assay was comparable to that obtained by 443
through UV spectrophotometry. Since any errors 444
in the UV assay will be reflected in the NIR 445
calibration, the equivalent R.S.D. are not surpris- 446
ing. The NIR assay is capable of determining the 447
active content within the accepted limits of 90– 448
110%. 449

Table 1

Content uniformity of testosterone in 3/8 in. TFCs disks as determined by the UV analysis method

Theoretical weight (mg)	0	1	2	3	4
Sample 1	0.0143	1.0092	2.4144	3.4158	3.7642
Sample 2	0.0228	1.0714	1.9484	3.4922	3.5163
Sample 3	0.0181	1.0463	1.9823	4.2133	3.7302
Sample 4	0.0219	1.0501	2.1848	3.6121	3.4775
Sample 5	0.0190	0.9942	2.3428	3.8369	4.7130
Mean \pm S.D.	0.0192 \pm 0.003	1.0343 \pm 0.032	2.1746 \pm 0.209	3.7141 \pm 0.321	3.8402 \pm 0.504
% R.S.D.	17.45	3.06	9.59	8.65	13.12

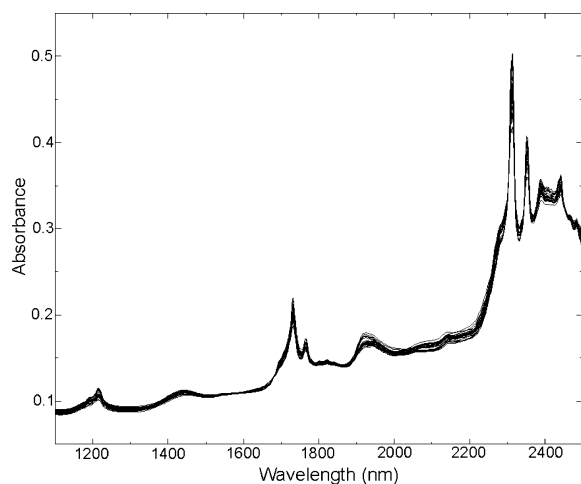


Fig. 3. Scatter-corrected NIR spectra of 3/8 in. TFCs containing testosterone. NIR was completed using a Technicon InfraAlyzer 500 (Tarrytown, NY). Scans were performed in the range of 1100–2500 nm.

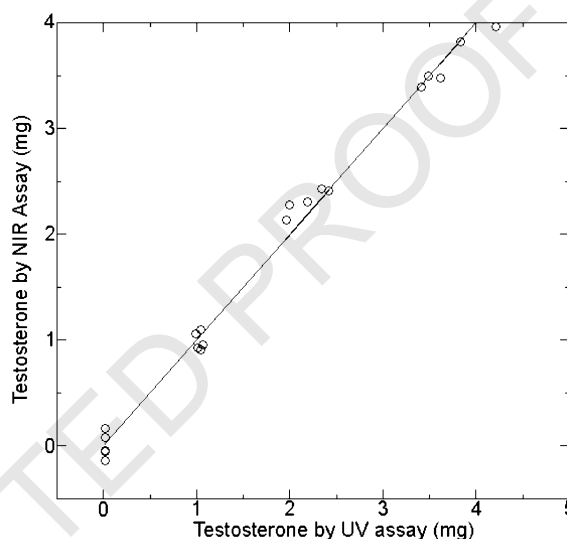


Fig. 4. Comparison of UV analytical method to the NIR analytical method in determining the content uniformity of testosterone in 3/8 in. TFCs (0–4 mg testosterone label strength). Validation samples are shown superimposed on the calibration line.

450 In conclusion, although the UV assay showed a
 451 slightly better r^2 value, the NIR assay was much
 452 quicker, easier, and nondestructive. The difference
 453 between $r^2 = 0.99$ for the NIR assay and $r^2 = 0.999$
 454 for the UV assay corresponds to a change in SEE
 455 of approximately 0.18–0.17 mg, a trivial difference
 456 over the 0–4 mg calibration range. Patches could
 457 be doubled up to increase path length, and such a
 458 technique might enable a useful calibration func-
 459 tion to be created in a lower concentration range
 460 (e.g. 0–1 mg testosterone). The NIR assay may
 461 have significant potential for use in the quality

control of pharmaceutical films containing testos- 462
 terone. 463

Acknowledgements 464

The work was supported, in part, by a grant 465
 from the Pharmaceutical Research and Manufac- 466
 turers of America Foundation 2001 Undergradu- 467
 ate Research Fellowship in Pharmaceutics to 468
 support the research of William Fountain. 469

References

- 470
471
472
473
474
475
476
477
478
479
480
481
482
483
484
485
486
487
488
489
490
491
492
493
494
495
496
497
498
499
500
501
502
503
504
505
506
507
508
509
510
511
512
513
514
515
516
517
518
519
520
521
522
523
524
- [1] J.D. Kirsch, J.K. Drennen, Nondestructive tablet hardness testing by near-infrared spectroscopy: a new and robust spectral best-fit algorithm, *J. Pharm. Biomed. Anal.* 19 (1999) 351–362.
- [2] J.D. Wargo, J.K. Drennen, Near-infrared spectroscopic characterization of pharmaceutical powder blends, *J. Pharm. Biomed. Anal.* 14 (1996) 1415–1423.
- [3] J.D. Kirsch, J.K. Drennen, Determination of film-coated tablet parameters by near-infrared spectroscopy, *J. Pharm. Biomed. Anal.* 13 (1995) 1273–1281.
- [4] G. Buckton, E. Yonemochi, W.L. Yoon, A.C. Moffat, Water sorption and near IR spectroscopy to study the differences between microcrystalline cellulose and silicified microcrystalline cellulose before and after wet granulation, *Int. J. Pharm.* 181 (1999) 41–47.
- [5] L. Allen, Quantitative determination of carisoprodol, phenacetin, and caffeine in tablets by near-IR spectrometry and their identification by TLC, *J. Pharm. Sci.* 63 (1974) 912–916.
- [6] A.S. Hussain, The process analytical technology (PAT) initiative: progress report and next steps, Process Analytical Technologies Subcommittee of the Advisory Committee for Pharmaceutical Science, Food and Drug Administration, June 12, 2002, Briefing <http://www.fda.gov/ohrms/dockets/ac/02/briefing/3869b1.htm>.
- [7] R.A. Lodder, G.M. Hieftje, Analysis of intact tablets by near-infrared reflectance spectrometry, *Appl. Spectrosc.* 42 (1988) 556–558.
- [8] R.A. Lodder, M. Selby, G.M. Hieftje, Detection of capsule tampering by near-infrared reflectance analysis, *Anal. Chem.* 59 (1987) 1921–1930.
- [9] R.A. Lodder, G.M. Hieftje, Detection of subpopulations in near-infrared reflectance analysis, *Appl. Spectrosc.* 42 (1988) 1500–1512.
- [10] P.K. Aldridge, R.F. Mushinsky, M.M. Andino, C.L. Evans, Identification of tablet formulations inside blister packages by near infrared spectroscopy, *Appl. Spectrosc.* 48 (1994) 1272–1276.
- [11] J.K. Drennen, R.A. Lodder, Nondestructive near-infrared analysis of intact tablets for determination of degradation product, *J. Pharm. Sci.* 79 (1990) 622–627.
- [12] T.M. Niemczyk, M.M. Delgado-Lopez, F.S. Allen, Quantitative determination of bucindolol concentration in intact gel capsules using Raman spectroscopy, *Anal. Chem.* 70 (1998) 2762–2765.
- [13] R.J. Dempsey, D.G. Davis, R.G. Buice, Jr, R.A. Lodder, Biological and medical applications of near-infrared spectrometry, *Appl. Spectrosc.* 50 (1996) 18A–34A.
- [14] M. Fischer, C.D. Tran, Investigation of solid-phase peptide synthesis by the near-infrared multispectral imaging technique: a detection method for combinatorial chemistry, *Anal. Chem.* 71 (1999) 2255–2261.
- [15] M. Fischer, C.D. Tran, Evidence for kinetic inhomogeneity in the curing of epoxy using the near-infrared multispectral imaging technique, *Anal. Chem.* 71 (1999) 953–959.
- [16] C.D. Tran, Y. Cui, S. Smirnov, Simultaneous multispectral imaging in the visible and near-infrared region: applications in document authentication and determination of chemical inhomogeneity of copolymers, *Anal. Chem.* 70 (1998) 4701–4708.
- [17] S. Jay, W. Fountain, Z. Cui, R.J. Mumper, Transmucosal delivery of testosterone in rabbits using novel bi-layer mucoadhesive wax-film composite disks, *J. Pharm. Sci.* 91 (2002) 2016–2025.
- [18] Z. Cui, R.J. Mumper, Buccal transmucosal delivery of calcitonin in rabbits using thin-film composites, *Pharm. Res.* 19 (2002) 1901–1906.
- [19] Z. Cui, R.J. Mumper, Bi-layer films for mucosal (genetic) immunization via the buccal route in rabbits, *Pharm. Res.* 19 (2002) 947–953.
- [20] R.A. Lodder, G.M. Hieftje, A disposable liquid microcell for near-infrared reflectance analysis, *Appl. Spectrosc.* 42 (1988) 518–519.
- [21] A. Gambineri, R. Pasquali, Testosterone therapy in men: clinical and pharmacological perspectives, *J. Endocrinol. Invest.* 23 (2000) 196–214.
- [22] J.G. Rabkin, G.J. Wagner, R. Rabkin, A double-blind, placebo-controlled trial of testosterone therapy for HIV-positive men with hypogonadal symptoms, *Arch. Gen. Psychiatry* 57 (2000) 141–147.
- [23] S. Parker, M. Armitage, Experience with transdermal testosterone replacement therapy for hypogonadal men, *Clin. Endocrinol.* 50 (1999) 57–62.
- [24] J. Voorspoels, J.P. Remon, W. Eechaute, W. De Sy, Buccal absorption of testosterone and its esters using a bioadhesive tablet in dogs, *Pharm. Res.* 13 (1996) 1228–1232.
- [25] A.S. Dobs, D.R. Hoover, M.C. Chen, R. Allen, Pharmacokinetic characteristics, efficacy, and safety of buccal testosterone in hypogonadal males: a pilot study, *J. Clin. Endocrinol. Metab.* 83 (1998) 33–39.
- [26] S.J. Winters, Current status of testosterone replacement therapy in men, *Arch. Fam. Med.* 8 (1999) 257–263.
- [27] C.C. Slater, I. Souter, C. Zhang, C. Guan, F.Z. Stanczyk, D.R. Mishell, Pharmacokinetics of testosterone after percutaneous gel or buccal administration, *Fertil. Steril.* 76 (2001) 32–37.
- [28] S. Kim, W. Snipes, G.D. Hodgen, F. Anderson, Pharmacokinetics of a single dose of buccal testosterone, *Contraception* 52 (1995) 313–316.
- [29] C.B. Cutter, Compounded percutaneous testosterone gel: use and effects in hypogonadal men, *J. Am. Board Fam. Pract.* 14 (2001) 22–32.
- [30] W.P. Jordan, Allergy and topical irritation associated with transdermal testosterone administration: a comparison of scrotal and nonscrotal transdermal systems, *Am. J. Contact Dermatitis* 8 (1997) 103–113.
- [31] W.P. Jordan, L.E. Atkinson, Comparison of the skin irritation potential of two testosterone transdermal systems: an investigational system and a marketed product, *Clin. Ther.* 20 (1998) 80–87.
- 525
526
527
528
529
530
531
532
533
534
535
536
537
538
539
540
541
542
543
544
545
546
547
548
549
550
551
552
553
554
555
556
557
558
559
560
561
562
563
564
565
566
567
568
569
570
571
572
573
574
575
576
577
578
579
580
581

- 582 [32] A.S. Dobs, A.W. Meikle, S. Arver, S.W. Sanders, K.E. system in comparison with bi-weekly injections of testos- 585
583 Caramelli, N.A. Mazer, Pharmacokinetics, efficacy, and terone enanthate for the treatment of hypogonadal men, J. 586
584 safety of a permeation-enhanced testosterone transdermal Clin. Endocrinol. Metab. 84 (1999) 3469–3478. 587
588

UNCORRECTED PROOF